Published in final edited form as:
J Immunol. 2016 November 15; 197(10): 4042–4052. doi:10.4049/jimmunol.1601132.

HIV-1 Nef Impairs the Formation of Calcium Membrane Territories Controlling the Signaling Nanoarchitecture at the Immunological Synapse1

Joana G. Silva[1], **Nuno P. Martins**[2], **Ricardo Henriques**[3], and **Helena Soares**[1,*]

[1]Immunobiology and Pathogenesis Group, CEDOC-Chronic Diseases Research Center, NOVA Medical School| Faculdade de Ciências Médicas, NOVA University of Lisbon, Lisbon, Portugal

[2]Unit of Imaging and Cytometry, Instituto Gulbenkian de Ciência, Oeiras, Portugal

[3]Quantitative Imaging and Nanobiophysics Group, MRC Laboratory for Molecular Cell Biology and Department of Cell and Developmental Biology, University College London, London, United Kingdom

Abstract

The ability of HIV-1 to replicate and to establish long-term reservoirs is strongly influenced by T cell activation. By pioneering the use of membrane tethered genetically encoded calcium (Ca^{2+}) indicators we were able to detect, for the first time, the formation of Ca^{2+} territories and determine their role in coordinating the functional signaling nanostructure of the synaptic membrane. Consequently, we report a previously unknown immune subversion mechanism involving HIV-1 exploitation, through its Nef accessory protein, of the interconnectivity between three evolutionary conserved cellular processes: vesicle traffic, signaling compartmentalization and the second messenger Ca^{2+}. We found that HIV-1 Nef specifically associates with the traffic regulators MAL and Rab11b compelling the vesicular accumulation of Lck. Through its association with MAL and Rab11b, Nef co-opts Lck switch-like function driving the formation Ca^{2+} membrane territories, which in turn, control the fusion of LAT-transporting Rab27 and Rab37 vesicles and the formation of LAT nanoclusters at the immunological synapse. Consequently, HIV-1 Nef disengages TCR triggering from the generation of pLAT and pSLP nanoclusters driving TCR signal amplification and diversification. Altogether our results indicate that HIV-1 exploits the interconnectivity between vesicle traffic, Ca^{2+} membrane territories and signaling nanoclusters to modulate T cell signaling and function.

Introduction

The ability of HIV-1 to replicate in T cells is dependent on T cell activation state (1, 2). The accessory HIV-1 protein Nef enhances viral replication by modulating multiple signaling pathways through a plethora of interactions with cellular proteins (3). According to the

*Corresponding author: helena.soares@nms.unl.pt.

Author contributions statement

HS conceived the project. HS and RH designed experiments. JS, NP, RH and HS performed and analyzed experiments. HS wrote the paper and all the authors commented on it.

Europe PMC Funders Author Manuscripts

literature, Nef may interact with as many as 60 cellular factors and affect the function of more than 180 proteins (3). Notwithstanding, there is a pressing need to progress from this encyclopaedic listing of Nef interactions into a more conceptual approach and determine how Nef intersects the regulatory mechanisms controlling the activation and/or differentiation state of the infected cell. T cell activation is coordinated at a specialized interface that forms upon contact with an antigen-presenting cell, known as immunological synapse. TCR triggering induces the recruitment and activation of the kinases Lck and ZAP70, which in turn phosphorylates LAT. Phosphorylated LAT recruitment of SLP76 allows for the formation of a signaling supramolecular scaffold, nucleating various signaling complexes involved in remodeling the T cell cytoskeleton (4), T cell development (5) and activation (6). Thus, the assembly of LAT-SLP76 signaling complexes, also called the “LAT signalosome” is critical for T cell activation. The vesicular traffic has emerged as a central player in the assembly of the signaling machinery at the immunological synapse (7).

The TCR as well as the membrane-associated Lck and LAT signaling molecules exploit the vesicular traffic to concentrate at the immunological synapse (7). Recent works have started to address the molecular mechanisms that regulate the exocytic targeting of different vesicular compartments at the immunological synapse (8–10).

Along these lines, we have determined that the regulated release of LAT vesicles to the immunological synapse determines the functional nanostructure of the synaptic membrane and the coordination of the immune response (7, 8). We showed that Lck acts as the signal switch and Ca^{2+} acts as the mediator of a vesicle fusion feedback loop that builds a functional immunological synapse capable of driving T cell activation and cytokine production (8). Thus deciphering the spatial organization of signaling proteins is not only key to understand the mechanisms that underlie immune cell activation, but also to identify common design principals that are likely to be co-opted by HIV-1.

In this work we aimed at deciphering molecular mechanisms underpinning the control of T cell activation in order to identify the common design principals that are likely to be co-opted by HIV infection. We uncovered a previously unknown immune subversion mechanism involving HIV-1 exploitation, through its Nef accessory protein, of the interconnectivity between three evolutionary conserved cellular processes: vesicle traffic, signaling compartmentalization and the second messenger Ca^{2+}. We found that Nef selectively interacts with Lck vesicle traffic regulators Rab11b and MAL restraining Lck from the immunological synapse. We pioneered the use of membrane tethered genetically encoded Ca^{2+} indicators (11) to detect and characterize the formation of Ca^{2+} territories at the TCR stimulated membrane. Interestingly, we determined that Nef impairs the formation of Ca^{2+} membrane territories at the immunological synapse even though it has no effect on cytosolic Ca^{2+} fluxes (12). Finally, by restraining Lck away from the immunological synapse, Nef co-opts the switch regulatory function of synaptic Lck in promoting the generation of Ca^{2+} membrane territories controlling LAT vesicle fusion and the signaling nanoarchitecture of the immunological synapse.

Materials and Methods

Vectors and Transfection

Lck_{MA}-LAT-GFP and LAT_{TM}-Lck-GFP were constructed by PCR-fusion of the Lck kinase aminoacids 1-18 and LAT aminoacids 28-262 and of the LAT aminoacids 1-27 and Lck aminoacids 19-501, respectively. pN1-Fyn-GCaMP3 was obtained by replacing the membrane targeting sequence of Lck with the one of Fyn, through Gibson assembly, on pN1-Lck-GCaMP3 construct obtained from Adgene through Gibson Assembly. The construct of Nef allele NL4.3 and its mutants fused to GFP or mCherry were gifts from F. Niedergang (Institut Cochin, Paris, France). The Gts-Nef (revGlc-NefΔSH4) and Fyn_{MA}-Lck-GFP (FynN18-Lck.GFP) constructs were provided by O.T. Fackler (University Hospital Heidelberg, Heidelberg, Germany), the latter was used to clone Fyn_{MA}-Lck-mCherry. The MAL-GFP construct was a gift from M. A. Alonso (Universidad Autonoma de Madrid, Madrid, Spain); the Rab11b-GFP and Rab27-GFP constructs were a gift from D. Barral (CEDOC- Chronic Diseases Research Center, Lisbon, Portugal), and the Rab37-GFP construct was a gift from B. Goud (Institut Couchin, Paris, France). DNA constructs were inserted into Jurkat and primary CD4 T cells using Invitrogen Neon Transfection system. Transiently transfected cells were analyzed 24 h after transfection. Primary CD4 T cells were transfected once with siRNA oligonucleotide pools (Invitrogen) targeting Lck. Silenced cells were analyzed 72 h after transfection.

Virus production and infection

To generate viral stocks, 293T cells were transfected with the HIV-1 NL4.3 and HIV-1 NL4.3 ΔNef constructs. Jurkat cells were infected with HIV-1 NL4.3 and HIV-1 NL4.3 ΔNef virus for 3 days prior to imaging as described before (13).

Cells, reagents and immunofluorescence

Jurkat cells clones E6.1 and $Lck^{-/-}$ Jurkat JCAM1.6 cells were grown in complete RPMI medium containing 10% (vol/vol) fetal bovine serum, nonessential aminoacids and L-glutamine. Human peripheral blood cells were stimulated with PHA (1 mg/ml) and grown for 7 days in RPMI 1640 medium with 10% FCS and 20 IU/ml IL-2. Glass coverslips coated with polylysine overnight at 4°C and, when stated, further incubated with stimulatory (αCD3 MEM-92; EXBIO and CD28; Genetech) or non-stimulatory (αCD45 mAb GAP 8.3; ATCC) antibodies at concentration of 10 μg/ml overnight at 4°C, as previously described (8). In some cases thapsigargin (5 μM; TPS) was added during the stimulation period. For imaging of Fyn-CaGMP3 transfected cells were imaged on RPMI medium at 37C. For all other conditions cells were then fixed with 4% paraformaldehyde for 30 min at room temperature, incubated with blocking buffer (PBS BSA 1%) with or without 0.05% saponin and stained with primary antibodies against Lck (3A5; Santa Cruz), LAT and pLAT (Cell Signaling), pSLP (J141; BD Biosciences), CD45 (GAP 8.3; ATCC), HA (ab9110 and ab18181; Abcam), and Gag (NIH AIDS reagent program) for 1 hour, washed and incubated for 45 min with Alexa 568 and Alexa 647 conjugated secondary antibodies (Life Technologies).

Imaging, image processing and quantification

Confocal images were obtained using a Zeiss LSM 710 confocal microscope (Carl Zeiss) over a 63x objective. 3D image deconvolution was performed using Huygens Essential (version 3.0, Scientific Volume Imaging), and 2D images were generated from a maximum intensity projection over a 3D volume cut of 1 μm depth centered either on the intracellular compartment when visible or on the cell center. For the quantification of Lck and LAT subcellular distribution the plasma membrane of CD4 T cells was surface labeled with anti-CD45 mAbs. Plasma membrane segmentation was implemented through the generation of binary mask delimitating the internal and external outlines of the plasma membrane using the Fiji image analysis software.

FRET imaging

A first set of FRET-donor (GFP tagged proteins) and FRET-acceptor (mCherry tagged proteins) confocal images were acquired at low excitation intensity. Acceptor photobleaching with a 561 nm laser was then carried out through strong illumination of a region-of-interest (ROI) corresponding to the intracellular compartment of each cell. mCherry showed 90% decrease in signal within the defined ROI. A second set of images was acquired at low excitation intensity after acceptor photobleaching. Both pre-bleaching and post-bleaching datasets were corrected for drift and analyzed with the AccPbFRET plugin for ImageJ software (Graphpad)

*d*STORM Imaging

Glass coverslips were washed 2-3 times in optical grade acetone, soaked overnight and sonicated in 0.1M KOH for 20 min. Coverslips were then thoroughly rinsed in deionized water and dried. The glass coverslips were coated overnight at room temperature with 0.001 % poly-L-Lysine (Sigma) diluted in PBS. Dried coverslips were subsequently incubated with stimulatory (αCD3 MEM-92; EXBIO and CD28; Genetech) or non-stimulatory (αCD45 mAb GAP 8.3; ATCC) antibodies at concentration of 10 μg/ml overnight at 4°C. Cells were resuspended in imaging buffer, and 500,000 cells were dropped onto the coverslips and incubated for 5 min at 37°C. In some cases thapsigargin (5 μM) was added during the incubation period. Cells were then fixed with 4% paraformaldehyde for 30 min at room temperature. In order to maximize the number of detected molecules care was taken to minimize photobleaching: cells were embedded in oxygen scavenger buffer, imaged on the same day of labeling and kept in the dark until imaged. *d*STORM images were then acquired with a Nikon Ti microscope coupled with a Hamamatsu Flash Orca 4.0 sCMOS camera and a 100x Plan Apo λ 1.45NA oil immersion objective at a 50 Hz rate. 561nm (Coherent Genesis MX 561-500 STM) and 638nm (Vortran Stradus 642-110) wavelength lasers lines were used to excite Alexa Fluor 568 and Alexa Fluor 647, respectively, using emission filters 595/50 and 655LP from Chroma Technology Corp. to further reduce and limit crosstalk. For a better signal to noise ratio, a pseudo-TIRF illumination (oblique illumination) was used. Acquisition was done through μManager freeware (14) and acquired data was then processed and reconstructed through Fiji (15) using super-resolution plugin ThunderSTORM (16).Once events were detected, a data table was exported with x-y coordinates of each molecule, photon count and spatial precision, which could later be

converted into an image. These data sets were then processed to check for possible cluster formation.

For spatial point pattern of molecular detection, Ripley's K-function was then calculated through a Fiji macro of commands as followed:

For $i \neq j$

$$K(r)=A\sum_{i=1}^{n}\sum_{j=1}^{n}\left(\frac{\delta_{ij}}{n^2}\right) \; where \; \delta_{ij}=1 \; if \; \delta_{ij}<r, otherwise \; 0$$

Were A is the area of the analyzed region (which depends on the radius), r is the radius of the analyzed area, n is the number of detected particles and δ is the distance between points i and j. This counts the number of molecules inside the circle area around each detected particle and normalizes it to the average molecular density of all areas measured to access possible cluster formation.

Flow cytometry

Jurkat cells were stained with FITC-labeled mAbs against CD4 (RPA-T4, BD Biosciences) and with unconjugated mAbs against HA (ab9110, Abcam) followed by incubation with Alexa 647-labelled anti-rabbit Ab (Life Technologies). Cell-associated fluorescence was collected on a FACS Calibur and analyzed using the Flow Jo software (BD Biosciences). For Ca^{2+} flow measurements, Jurkat cells (5.10^6/ml) resuspended in phenol red free RPMI 1640 were loaded with 1mM of Indo-1 (Molecular Probes) at 37ºC in the dark for 45 min. Cells were washed and resuspended in the same medium. Ca^{2+} measurements were performed on a MoFlo flow cytometer (Beckman Coulter). Cells were acquired for 90 sec to establish the base line followed by ionomycin addition (10 μg/ml). A ratiometric analysis was performed using the Flow Jo software (BD Biosciencies)

Results

The N-terminus of HIV-1 Nef promotes the selective accumulation of Lck, but not LAT, in the vesicular compartment

In recent years, the vesicle traffic of signaling molecules has emerged as a central regulator of T cell activation (7–10). In particular, we have determined that the formation of nanoterritories where signaling is coordinated to promote T cell activation is regulated by a vesicular traffic amplification loop involving the sequential vesicle delivery of Lck and LAT at the immunological synapse (8). Even though the main determinant of HIV-1 pathogenesis is the modulation of TCR signaling by the viral protein Nef, it remains poorly understood how Nef exploits the interconnectivity between vesicular traffic and synaptic signaling underpinning T cell activation.

To address this open question, we started by determining the effect of Nef on Lck and LAT subcellular distribution (7). As previously reported, Nef retains Lck in an enlarged perinuclear vesicular compartment (7, 13, 17) (Fig. 1A, B), both in Jurkat and in primary

Europe PMC Funders Author Manuscripts

CD4 T cells (Fig. 1A, B). Unexpectedly, Nef does not alter the subcellular distribution of LAT, despite their adjacent localization in the tightly filled T cell cytoplasm (Fig. 1A, B).

To gain mechanistic insights on how Nef specifically alters Lck subcellular distribution, we tailored the expression of a large set of GFP tagged Lck and LAT chimeric proteins (Fig. 1C) and assessed their subcellular distribution (Fig. 1D, E). Previous works have reported that the biological activity of Nef is controlled by the specificity of its membrane targeting (18), but also that the Lck membrane anchoring domain, which encodes Lck traffic properties, is necessary and sufficient to undergo Nef-mediated retention (18). First, we confirmed that rerouting Nef to the Golgi compartment prevents Lck vesicular accumulation (Fig. 1A-C; Gts-Nef), underscoring the relevance of specific membrane targeting to Nef biological activity. Next, to clarify if the Lck membrane anchoring domain is necessary and sufficient to undergo Nef-mediated retention, we used a Lck construct encoding solely the membrane anchoring (MA) domain consisting of its first 18-aa and devoid of additional protein interaction surfaces fused to GFP (Lck_{MA}) and expressed it in Lck deficient $Lck^{-/-}$ JCAM1.6 cells. Co-transfection of Nef-mCherry and Lck_{MA}-GFP in $Lck^{-/-}$ JCAM1.6 cells caused the vesicular accumulation of the Lck_{MA}-GFP to the similar extent to the one verified with endogenous Lck (Fig. 1 A, B, D, E), confirming that the MA domain of Lck is sufficient to undergo Nef mediated vesicular accumulation (19).

Lck and the closely related Fyn kinase display distinct MA domains and consequently are segregated to distinct vesicular compartments (20). Since Nef does not alter the vesicular distribution of the closely related Fyn kinase (17), we then expressed in Jurkat T cells a chimeric protein with all the Lck functional motifs except for the MA domain, which has been replaced by the one of Fyn (Fig. 1C; Fyn_{MA}-Lck). Despite the presence of all the Lck interaction motifs in the Fyn_{MA}-Lck chimeric protein, Nef did not cause the vesicular accumulation of Fyn_{MA}-Lck (Fig. 1D, E).

We next interchanged Lck and LAT trafficking properties by constructing chimeric proteins in which the Lck MA domain was replaced by LAT transmembrane (TM) domain (Fig. 1C; LAT_{TM}-Lck) and the LAT TM domain was replaced by Lck MA domain (Fig. 1C; Lck_{MA}-LAT). Conferring LAT traffic properties to Lck abrogated its retention by Nef and reciprocally, endowing LAT with Lck traffic properties led to LAT vesicular accumulation in Nef expressing Jurkat cells (Fig. 1D, E).

These results indicate that N-terminus domain of Lck is required for its selective vesicular accumulation mediated by Nef.

HIV-1 Nef selectively associates with Lck traffic regulators

The specification of the vesicular identity and traffic route rely on the Rab family GTPases (21). Lck and LAT reside and traffic in distinct vesicular compartments, with little to no overlap in their Rab specification (8). While Lck localizes to Rab11b- and MAL-positive vesicles (8, 22, 23), LAT resides in vesicles marked with Rab27 and Rab37 (8). We transiently co-expressed each Rab-GFP protein with Nef-mCherry, in Jurkat and in primary T cells, and assessed their co-localization in the vesicular compartment. To exclude the possibility that Nef co-localization with MAL and Rab11b could be due to Nef interaction

with Lck (24, 25), we first investigated whether Nef co-localized preferentially with Lck traffic regulators, in $Lck^{-/-}$ JCAM1.6 and primary T cells (Fig. 2A). In both Jurkat and in primary T cells, Nef highly co-localized with Lck traffic regulators Rab11b and MAL (~80%, Fig. 2A-C) and only partially co-localized with Rab27 and Rab37 (~20%; Fig. 2A-C), even when Lck (LAT_{TM}-Lck) was targeted to LAT transporting Rab27 and Rab37 vesicles (~8%; Fig. 2A-C). Conversely, rerouting Nef to the Golgi (Gts-Nef) abolished its colocalization with Rab11b and MAL (~5%; Fig. 2A-C). Altogether, these results indicate that Lck vesicular accumulation requires Nef association with its traffic regulators Rab11b and MAL and that this association is established independently of Lck.

To analyze if Nef does in fact associate with Lck traffic regulators, we performed Fluorescence Resonance Energy Transfer (FRET) analysis through acceptor photobleaching (apFRET), which detects molecular proximities under 10 nm (26).

Nef associated with both Rab11b and MAL even in the absence of Lck (~20% FRET efficiency; Fig. 3A, B $Lck^{-/-}$ JCAM1.6). However, Nef did not associate with LAT traffic regulators Rab27 and Rab37 (~3% FRET efficiency; Fig. 3A, B Jurkat cells). Consistent with our previous findings, rerouting Nef to the Golgi abolished Nef association with Lck traffic regulators Rab11b and MAL (~2% FRET efficiency; Fig. 3A, B Jurkat cells Gts-Nef).

These results show that HIV-1 Nef associates in situ Rab11b and MAL and that this association is supported by Nef traffic properties.

Nef co-opts the switch-like regulatory function of synaptic Lck in promoting the generation of LAT signaling nanoclusters

T cell activation relies on the generation of an amplification signalosome formed by direct association of phosphorylated LAT (pLAT) and SLP76 (pSLP76)-Gads complexes (27). Given that Lck synaptic clustering acts as the signal switch required for the formation of LAT signaling territories (8), we investigated whether the vesicular retention would impair the functional architecture of LAT signaling in Nef-expressing cells. We triggered T cell activation by incubating the T cells for 5, or 12 min on coverslips coated with antibodies to CD3 and CD28 followed by fixation. We visualized Nef effects on Lck and LAT vesicle release at the immunological synapse by 3D-confocal microscopy (Fig. 4; top panels) and we determined Nef alterations to the functional architecture of the synaptic membrane using dual-color *d*STORM combined with TIRF (Fig. 4; bottom panels) (28).

As expected, Nef expression or HIV-1 infection prevented the Lck vesicular compartment delivery at the immunological synapse (Fig. 4A, B, D; top panels). However, regardless of the fact that Nef does not interact with LAT vesicular traffic (Fig. 1 and 2), LAT vesicle delivery is also impaired in Nef expressing cells (Fig. 4A, B, D; top panels). Regarding the signaling architecture of activated T cells, we observed that both Nef and HIV-1 infection reduced the number and size of signaling active pLAT nanoclusters at the immunological synapse (Fig 4B, D, G, H) as well as their capacity to recruit and form signaling complexes with pSLP76 (Fig. 4B, D, I, J). All of these defects were rescued when T cells were infected with a Nef-deleted virus (HIV-ΔNef; Fig. 4E-J), but not by stimulating HIV-1 infected cells

for longer (12' HIV; Fig. 4F-J). This indicates that the signaling deficit in HIV-1 infected cells is unlikely to be a manifestation of delayed kinetics.

These data suggest that, by retaining Lck in a vesicular compartment, Nef impairs the vesicle fusion positive feed back loop that drives the formation of pLAT nanoclusters at the immunological synapse. To formally test this hypothesis, we recovered Lck clustering at the immunological synapse of Nef-expressing cells by co-expressing the chimeric Fyn_{MA}-Lck protein whose traffic is not affected by Nef (Fig 1C, D). Fyn_{MA}-Lck expression completely recovered LAT vesicle delivery (Fig. 4C; top panel), the number and size of pLAT nanoclusters as well as their ability to recruit pSLP76 (Fig. 4C, G-J).

Our results collectively demonstrate that, by retaining Lck in a vesicular compartment, Nef impairs the vesicle fusion positive feed back loop that drives the formation of pLAT nanoclusters and the subsequent recruitment of pSLP76.

HIV-1 Nef impairs the formation of the Ca^{2+} membrane territories

Given that Lck clustering might participate in organizing TCR signaling (8, 29) possibly via local Ca^{2+} fluxes (8, 30), we investigated the impact of HIV-1 Nef on the formation of Ca^{2+} domains following TCR engagement. We reasoned that if membrane localized Ca^{2+} are indeed determinant for the signaling architecture of the immunological synapse, the formation of Ca^{2+} territories should be detectable in TCR stimulated membrane. To pursue our hypothesis, we constructed a membrane tethered genetically encoded Ca^{2+}-sensor Fyn-$GCaMP_3$, whose membrane localization could not be altered by HIV-1 Nef (11). Our experimental set-up enabled us to directly detect the formation of Ca^{2+} territories at the synaptic membrane, by measuring the increase in Fyn-$GCaMP_3$ fluorescence intensity. TCR engagement, by incubating the T cells on coverslips coated with antibodies to CD3 and CD28 promoted the formation of Ca^{2+} territories at the membrane of control and HIV-ΔNef infected cells T cells, but not of Nef-expressing or HIV-infected cells (Fig. 5A, B). Interestingly, co-expressing of Fyn_{MA}-Lck and Nef reverted the formation of Ca^{2+} territories at the stimulatory membrane, indicating that Lck signaling at the immunological synapse is required for the formation of Ca^{2+} territories. Finally, Nef-expressing cells exhibited no intrinsic functional defect in the Ca^{2+} channels, since treatment with Ca^{2+} flux inducing drugs thapsigargin and ionomycin restored the formation of Ca^{2+} territories at the synaptic membrane of Nef-expressing cells and also induced similar cytosolic levels of Ca^{2+} influx, respectively (Fig. 5A-C).

These data indicate that HIV-1 impairs the formation of Ca^{2+} territories at the synaptic membrane by removing Lck from the immunological synapse.

HIV-1 Nef impairs the formation of calcium territories orchestrating the signaling nanoarchitecture at the synaptic membrane

Finally, to assess the direct impact of Nef on the orchestration of TCR signaling nanoarchitecture, we determined the effect of impaired Ca^{2+} territories on LAT vesicle docking and/or fusion at the synaptic membrane. LAT vesicles are decorated by the exocytic Rab27 and Rab37, by the v-SNARE Ti-VAMP and by the Ca^{2+} sensor synaptotagmin-7 which mediate docking and/or fusion of vesicles with target membranes (8, 9, 21, 31). To

distinguish between vesicle docking and vesicle fusion, we used a engineered LAT molecule with an extracellular hemagglutinin (HA) tag that allows for surface labeling of LAT (LAT-HA) (9). Population comparison of HA labeling of control and Nef co-transfected T cells by flow cytometry and by confocal microscopy showed that both control and Nef co-transfected T cells expressed equivalent levels of LAT-HA (Fig. 6A) with similar subcellular distribution at the plasma membrane and within the vesicular compartment (Fig. 6B, C). Activation on coverslips coated with αCD3 and αCD28 antibodies of control and HIV-ΔNef infected T cells induced the fusion of the vesicular pool of LAT-HA at the synaptic membrane and the formation of LAT-HA nanoclusters measured by surface labeling (Fig. 6D, H), which were indistinguishable in number, size and density from endogenous pLAT nanoclusters (Figs. 4, 6D, H-J). These results indicate that LAT vesicle fusion is required for the orchestration of a LAT signaling nanoarchitecture. In Nef expressing or in HIV-infected cells there was a stark decrease in the number, size and density of surface LAT-HA, reflecting Nef impairment of LAT vesicle fusion at the synaptic membrane (Fig. 6E, G, I, J). Importantly, restoration of Ca^{2+} territories by thapsigargin treatment in αCD3 and αCD28 stimulated Nef-expressing cells completely recovered LAT-HA nanoclustering in number, size and density (Fig. 6F, I, J). These data collectively indicate that HIV-1 exploits the exquisite interconnectivity between Lck signaling and the formation of Ca^{2+} territories to impair the orchestration of a functional immunological synapse.

Discussion

Crosstalk between vesicle traffic, Ca^{2+} gradients and TCR signaling coordinates T cell activation (7, 32). Here, we report a previously unknown immune subversion mechanism involving HIV-1 Nef exploitation of the interconnectivity between vesicle traffic, Ca^{2+} membrane territories and TCR signaling. This inhibitory mechanism required Nef to co-opt Lck switch-like function driving the formation of Ca^{2+} membrane territories controlling the vesicular fusion amplification loop impelling LAT nanoclustering at the immunological synapse.

Nef has been characterized as a potent, multifunctional modulator of T cell activation (3). It is now accepted the central role of vesicular traffic in regulating the assembly of signaling complexes at the immunological synapse for T cell activation (7, 32, 33). We propose that Nef has evolved to co-opt the traffic checkpoints regulating the functional nanoarchitecture of the immunological synapse rather than by inhibiting a series of signaling molecules involved in sequential steps of TCR signaling cascade (34). We have found that Nef interacts with Lck traffic regulators, Rab11b and MAL, but not with LAT traffic regulators Rab27 and Rab37 (8, 22, 23). These interactions resulted in the selective retention of Lck in an enlarged vesicular compartment, in Nef-expressing cells. Interchanging Lck and LAT trafficking properties impaired Lck retention and reciprocally led to LAT vesicular accumulation in Nef expressing cells. We employed several different experimental approaches to determine if Nef interacts directly with MAL, however, the results of these experiments were inconclusive. One possible explanation for these inconsistences is that transmembrane proteins containing multiple hydrophobic domains, as is the case of MAL, often possess different tertiary structures and binding affinities when in solution relative to those occurring within a lipid bilayer. Such changes might confound solution-based analysis such as co-IP and far-Western

detection or even render physical interaction between Nef and MAL impossible in these conditions. On the other hand, FRET analysis performed under physiologic conditions with MAL in its native conformation within a lipid bilayer yielded that Nef and MAL are found at interacting distances. In fact, we detected Nef association with both Rab11b and MAL in Lck-deficient cells, precluding the possibility that Nef-Rab11b/MAL in situ interaction could be the result of a tripartite association between Lck-MAL/Rab11b-Nef. We found that rerouting of Nef trafficking from the Rab11+ MAL+ recycling compartment to the close by Golgi vesicles completely abolished Nef activity. Our results suggest that Nef-mediated Lck vesicular retention is the result of the specific Nef-membrane association to the Rab11b and MAL trafficking compartment. Consistent with our results, a recent study has found that Nef biological activity, including Lck vesicular accumulation, is supported by the specificity of its membrane anchoring domain (18). Curiously, a early work on Nef pathogenicity had found that the membrane anchoring domain of Nef was required for Nef mediated retention of Lck through the formation of a protein complex (25). Complimentary, we and others showed that Lck vesicular accumulation does not depend on its SH3 mediated interaction with Nef, requiring only Lck membrane anchoring domain (Lck_{MA}) (19). It is thus possible that by promoting Lck vesicular accumulation, Nef association with Rab11b and MAL facilitaes Nef modulation of Lck kinase activity through interaction with its SH3 domain.

Even though Nef motifs responsible for promoting the internalization and vesicular accumulation of the transferrin receptor (35), CD80/CD86 and MHCI(36) differ, all of these molecules share the striking commonality of trafficking through a Rab11b compartment. It is tempting to propose that once internalized, the transferrin receptor, CD80/CD86 and MHCI are prevented to recycle back to the plasma membrane as the consequence of Nef interaction with their common traffic regulator, Rab11b. Thus, Nef interaction with Rab11b reported in this study might allow for a unified view for the molecular mechanisms underpinning the vesicular retention of distinct molecules across distinct cell types (lymphocytes macrophages and dendritic cells) and might provide valuable insight into Rab11b role in HIV-1 budding (37).

The spatial organization of signaling proteins determines the T cell activation outcome (7–10, 32, 38, 39). Thus, to understand Nef modulation of T cell activation it is imperative to move from simply identifying the individual TCR signaling molecules targeted by Nef into determining the molecular mechanism underpinning Nef co-opt of the spatial organization of signaling components. Super-Resolution microscopy has made important contributions towards revealing the molecular mechanisms controlling the signaling nano-architecture of the immunological synapse (8–10, 38, 39). By combining dual-color *dSTORM* with TIRF microscopy, we found that by interfering with the MAL-mediated route of Lck transport, Nef disengages TCR triggering from LAT vesicle fusion and alters LAT signaling nano-architecture at the synaptic membrane. Accordingly, Nef expression decreased the number, density and size of pLAT nanoclusters. The formation of elongated TCR signaling nanoclusters has been positively correlated with the efficiency of signal transmission (8, 38, 40). Interestingly, we noted a shift in the synaptic signaling pattern of Nef-expressing cells from the elongated nanoclusters, observed in control cells, towards circular pLAT, which correlated with a decreased ability of pLAT to recruit pSLP76 and the consequent impaired assembly of the “LAT signalosome”. Finally, bypassing Lck vesicular retention was

Europe PMC Funders Author Manuscripts

sufficient to rescue pLAT nanoclustering at the immunological synapse of Nef-expressing cells. Further reinforcing that Nef impairment of LAT synaptic delivery is not the consequence of a direct interaction, but rather the consequence of Nef co-opting the switch-like regulatory function of synaptic Lck in promoting the vesicle fusion and the consequent formation of pLAT nanoclusters.

Lck clustering has been implicated in the organization of TCR signaling (8, 29) possibly via local Ca^{2+} fluxes (8, 30). Thus, by retaining Lck, Nef must impair the reorganization of the synaptic membrane that allows for the fusion of LAT vesicles. To map the impact of Nef on the formation of Ca^{2+} domains at the synaptic membrane, we pioneered the use of genetically encoded membrane tethered Ca^{2+} indicators (11), which detects highly localized Ca^{2+} signals that soluble probes fail to detect, to map the impact of Nef on the formation of Ca^{2+} domains at the synaptic membrane. Nef impairs the formation of Ca^{2+} membrane territories at the synaptic membrane even though it has no effect on cytosolic Ca^{2+} fluxes (12). Once again bypassing Lck vesicular retention was sufficient to rescue the formation of Ca^{2+} membrane territories at the TCR stimulated membrane, in Nef-expressing cells. These results illustrate the exquisite control that Nef exerts on the subcellular distribution of Ca^{2+} levels. While intracellular Ca^{2+} controls a remarkable breadth of cellular processes, including secretion, motility and differentiation, local Ca^{2+} domains are essential to regulate specific signaling events(41–43). Thus by impairing the formation of Ca^{2+} territories at the stimulated membrane, Nef can block the feedback loop amplifying TCR signaling and lower T cell sensitivity to antigen without affecting other Ca^{2+} dependent functions that might be required for HIV-1 propagation. Impairment of Ca^{2+} membrane territories is possibly involved in Nef inhibition of other cellular processes, such as migration (44, 45) and phagocytosis (46), which might need to be reinterpreted accordingly.

In conclusion, this work shows that Nef has evolved to co-opt the traffic checkpoints regulating the functional nanoarchitecture of the immunological synapse. Obviously, alterations to the regulatory mechanisms controlling T cell signaling thresholds and signal amplification could underpin the establishment of long-term reservoirs. Thus, the provision of such a mechanism is necessary to identify molecular targets for the development of more efficient anti-viral therapies.

Acknowledgements

We are thankful to Nuno Moreno for his contribution in setting up the super-resolution microscope, to Cláudia Campos and Vasco Barreto for their help in cloning and to Cláudia Bispo for her help in intracellular calcium assay. We thank the NIH AIDS reagent program for providing the HIV-1 NL4.3 and HIV-1 NL4.3 ΔNef constructs, the antibody against Gag and the human IL-2.

[1] HS is supported by FCT under the FCT Investigator Programme and by iNOVA4Health (UID/Multi/04462/2013). RH funded by grants from the Biotechnology and Biological Sciences Research Council (BB/M022374/1) and Medical Research Council (MR/K015826/1).

References

1. Nabel G, Baltimore D. An inducible transcription factor activates expression of human immunodeficiency virus in T cells. Nature. 1987; 326:711–713. [PubMed: 3031512]

2. Stevenson M, Stanwick TL, Dempsey MP, Lamonica CA. HIV-1 replication is controlled at the level of T cell activation and proviral integration. EMBO J. 1990; 9:1551–1560. [PubMed: 2184033]
3. Arhel NJ, Kirchhoff F. Implications of Nef: host cell interactions in viral persistence and progression to AIDS. Curr Top Microbiol Immunol. 2009; 339:147–175. [PubMed: 20012528]
4. Bunnell SC, Kapoor V, Trible RP, Zhang W, Samelson LE. Dynamic actin polymerization drives T cell receptor-induced spreading: a role for the signal transduction adaptor LAT. Immunity. 2001; 14:315–329. [PubMed: 11290340]
5. Zhang W, Sommers CL, Burshtyn DN, Stebbins CC, DeJarnette JB, Trible RP, Grinberg A, Tsay HC, Jacobs HM, Kessler CM, Long EO, et al. Essential role of LAT in T cell development. Immunity. 1999; 10:323–332. [PubMed: 10204488]
6. Zhang W, Sloan-Lancaster J, Kitchen J, Trible RP, Samelson LE. LAT: the ZAP-70 tyrosine kinase substrate that links T cell receptor to cellular activation. Cell. 1998; 92:83–92. [PubMed: 9489702]
7. Soares H, Lasserre R, Alcover A. Orchestrating cytoskeleton and intracellular vesicle traffic to build functional immunological synapses. Immunol Rev. 2013; 256:118–132. [PubMed: 24117817]
8. Soares H, Henriques R, Sachse M, Ventimiglia L, Alonso MA, Zimmer C, Thoulouze M-I, Alcover A. Regulated vesicle fusion generates signaling nanoterritories that control T cell activation at the immunological synapse. J Exp Med. 2013; 210:2415–2433. [PubMed: 24101378]
9. Larghi P, Williamson DJ, Carpier J-M, Dogniaux S, Chemin K, Bohineust A, Danglot L, Gaus K, Galli T, Hivroz C. VAMP7 controls T cell activation by regulating the recruitment and phosphorylation of vesicular Lat at TCR-activation sites. Nat Immunol. 2013; 14:723–731. [PubMed: 23666293]
10. Williamson DJ, Owen DM, Rossy J, Magenau A, Wehrmann M, Gooding JJ, Gaus K. Pre-existing clusters of the adaptor Lat do not participate in early T cell signaling events. Nat Immunol. 2011; 12:655–662. [PubMed: 21642986]
11. Shigetomi E, Bushong EA, Haustein MD, Tong X, Jackson-Weaver O, Kracun S, Xu J, Sofroniew MV, Ellisman MH, Khakh BS. Imaging calcium microdomains within entire astrocyte territories and endfeet with GCaMPs expressed using adeno-associated viruses. The Journal of General Physiology. 2013; 141:633–647. [PubMed: 23589582]
12. Manninen A, Saksela K. HIV-1 Nef interacts with inositol trisphosphate receptor to activate calcium signaling in T cells. J Exp Med. 2002; 195:1023–1032. [PubMed: 11956293]
13. Thoulouze M-I, Sol-Foulon N, Blanchet F, Dautry-Varsat A, Schwartz O, Alcover A. Human immunodeficiency virus type-1 infection impairs the formation of the immunological synapse. Immunity. 2006; 24:547–561. [PubMed: 16713973]
14. Edelstein AD, Tsuchida MA, Amodaj N, Pinkard H, Vale RD, Stuurman N. Advanced methods of microscope control using μManager software. J Biol Methods. 2014; 1:10–10.
15. Schindelin J, Arganda-Carreras I, Frise E, Kaynig V, Longair M, Pietzsch T, Preibisch S, Rueden C, Saalfeld S, Schmid B, Tinevez J-Y, et al. Fiji: an open-source platform for biological-image analysis. Nat Meth. 2012; 9:676–682.
16. Ovesný M, Křížek P, Borkovec J, Svindrych Z, Hagen GM. ThunderSTORM: a comprehensive ImageJ plug-in for PALM and STORM data analysis and super-resolution imaging. Bioinformatics. 2014; 30:2389–2390. [PubMed: 24771516]
17. Pan X, Rudolph JM, Abraham L, Habermann A, Haller C, Krijnse-Locker J, Fackler OT. HIV-1 Nef compensates for disorganization of the immunological synapse by inducing trans-Golgi network-associated Lck signaling. Blood. 2012; 119:786–797. [PubMed: 22123847]
18. Geist MM, Pan X, Bender S, Bartenschlager R, Nickel W, Fackler OT. Heterologous Src homology 4 domains support membrane anchoring and biological activity of HIV-1 Nef. J Biol Chem. 2014; 289:14030–14044. [PubMed: 24706755]
19. Pan X, Geist MM, Rudolph JM, Nickel W, Fackler OT. HIV-1 Nef disrupts membrane-microdomain-associated anterograde transport for plasma membrane delivery of selected Src family kinases. Cell Microbiol. 2013; 15:1605–1621. [PubMed: 23601552]
20. Ley SC, Marsh M, Bebbington CR, Proudfoot K, Jordan P. Distinct intracellular localization of Lck and Fyn protein tyrosine kinases in human T lymphocytes. J Cell Biol. 1994; 125:639–649. [PubMed: 7513706]

21. Fukuda M. Regulation of secretory vesicle traffic by Rab small GTPases. Cell Mol Life Sci. 2008; 65:2801–2813. [PubMed: 18726178]
22. Gorska MM, Liang Q, Karim Z, Alam R. Uncoordinated 119 Protein Controls Trafficking of Lck via the Rab11 Endosome and Is Critical for Immunological Synapse Formation. The Journal of Immunology. 2009; 183:1675–1684. [PubMed: 19592652]
23. Anton O, Batista A, Millan J, Andres-Delgado L, Puertollano R, Correas I, Alonso MA. An essential role for the MAL protein in targeting Lck to the plasma membrane of human T lymphocytes. J Exp Med. 2008; 205:3201–3213. [PubMed: 19064697]
24. Collette Y, Dutartre H, Benziane A, Ramos-Morales, Benarous R, Harris M, Olive D. Physical and functional interaction of Nef with Lck. HIV-1 Nef-induced T-cell signaling defects. J Biol Chem. 1996; 271:6333–6341. [PubMed: 8626429]
25. Baur AS, Sass G, Laffert B, Willbold D, Cheng-Mayer C, Peterlin BM. The N-terminus of Nef from HIV-1/SIV associates with a protein complex containing Lck and a serine kinase. Immunity. 1997; 6:283–291. [PubMed: 9075929]
26. Wouters FS, Bastiaens PI, Wirtz KW, Jovin TM. FRET microscopy demonstrates molecular association of non-specific lipid transfer protein (nsL-TP) with fatty acid oxidation enzymes in peroxisomes. EMBO J. 1998; 17:7179–7189. [PubMed: 9857175]
27. Acuto O, Bartolo VD, Michel F. Tailoring T-cell receptor signals by proximal negative feedback mechanisms. Nat Rev Immunol. 2008; 8:699–712. [PubMed: 18728635]
28. Heilemann M, van de Linde S, Schüttpelz M, Kasper R, Seefeldt B, Mukherjee A, Tinnefeld P, Sauer M. Subdiffraction-Resolution Fluorescence Imaging with Conventional Fluorescent Probes. Angew Chem Int Ed. 2008; 47:6172–6176.
29. Rossy J, Owen DM, Williamson DJ, Yang Z, Gaus K. Conformational states of the kinase Lck regulate clustering in early T cell signaling. Nat Immunol. 2012; 14:82–89. [PubMed: 23202272]
30. Shi X, Bi Y, Yang W, Guo X, Jiang Y, Wan C, Li L, Bai Y, Guo J, Wang Y, Chen X, et al. Ca2+ regulates T-cell receptor activation by modulating the charge property of lipids. Nature. 2012; 493:111–115. [PubMed: 23201688]
31. Chaineau M, Danglot L, Galli T. Multiple roles of the vesicular-SNARE TI-VAMP in post-Golgi and endosomal trafficking. FEBS Lett. 2009; 583:3817–3826. [PubMed: 19837067]
32. Finetti F, Onnis A, Baldari CT. Regulation of vesicular traffic at the T cell immune synapse: lessons from the primary cilium. Traffic. 2015; 16:241–249. [PubMed: 25393976]
33. Benzing C, Rossy J, Gaus K. Do signalling endosomes play a role in T cell activation? FEBS J. 2013; 280:5164–5176. [PubMed: 23834225]
34. Abraham L, Bankhead P, Pan X, Engel U, Fackler OT. HIV-1 Nef Limits Communication between Linker of Activated T Cells and SLP-76 To Reduce Formation of SLP-76-Signaling Microclusters following TCR Stimulation. The Journal of Immunology. 2012; 189:1898–1910. [PubMed: 22802418]
35. Madrid R, Janvier K, Hitchin D, Day J, Coleman S, Noviello C, Bouchet J, Benmerah A, Guatelli J, Benichou S. Nef-induced Alteration of the Early/Recycling Endosomal Compartment Correlates with Enhancement of HIV-1 Infectivity. J Biol Chem. 2005; 280:5032–5044. [PubMed: 15569681]
36. Chaudhry A, Das SR, Jameel S, George A, Bal V, Mayor S, Rath S. HIV-1 Nef Induces a Rab11-Dependent Routing of Endocytosed Immune Costimulatory Proteins CD80 and CD86 to the Golgi. Traffic. 2008; 9:1925–1935. [PubMed: 18764822]
37. Varthakavi V, Smith RM, Martin KL, Derdowski A, Lapierre LA, Goldenring JR, Spearman PR. The Pericentriolar Recycling Endosome Plays a Key Role in Vpu-mediated Enhancement of HIV-1 Particle Release. Traffic. 2005; 7:298–307.
38. Lillemeier BF, Mörtelmaier MA, Forstner MB, Huppa JB, Groves JT, Davis MM. TCR and Lat are expressed on separate protein islands on T cell membranes and concatenate during activation. Nat Immunol. 2009; 11:90–96. [PubMed: 20010844]
39. Sherman E, Barr V, Manley S, Patterson G, Balagopalan L, Akpan I, Regan CK, Merrill RK, Sommers Cl, Lippincott-Schwartz J, Samelson LE. Functional Nanoscale Organization of Signaling Molecules Downstream of the T Cell Antigen Receptor. Immunity. 2011; 35:705–720. [PubMed: 22055681]

40. Kumar R, Ferez M, Swamy M, Arechaga I, Rejas MT, Valpuesta JM, Schamel WWA, Alarcon B, van Santen HM. Increased Sensitivity of Antigen-Experienced T Cells through the Enrichment of Oligomeric T Cell Receptor Complexes. Immunity. 2011; 35:375–387. [PubMed: 21903423]

41. Willoughby D, Cooper DMF. Organization and Ca2+ Regulation of Adenylyl Cyclases in cAMP Microdomains. Physiological Reviews. 2007; 87:965–1010. [PubMed: 17615394]

42. Chang W-C, Di Capite J, Singaravelu K, Nelson C, Halse V, Parekh AB. Local Ca2+ influx through Ca2+ release-activated Ca2+ (CRAC) channels stimulates production of an intracellular messenger and an intercellular pro-inflammatory signal. J Biol Chem. 2008; 283:4622–4631. [PubMed: 18156181]

43. Di Capite J, Ng SW, Parekh AB. Decoding of Cytoplasmic Ca2+ Oscillations through the Spatial Signature Drives Gene Expression. Current Biology. 2009; 19:853–858. [PubMed: 19375314]

44. Choe EY. HIV Nef Inhibits T Cell Migration. Journal of Biological Chemistry. 2002; 277:46079–46084. [PubMed: 12354773]

45. Park IW, He JJ. HIV-1 Nef-mediated inhibition of T cell migration and its molecular determinants. Journal of Leukocyte Biology. 2009; 86:1171–1178. [PubMed: 19641037]

46. Mazzolini J, Herit F, Bouchet J, Benmerah A, Benichou S, Niedergang F. Inhibition of phagocytosis in HIV-1-infected macrophages relies on Nef-dependent alteration of focal delivery of recycling compartments. Blood. 2010; 115:4226–4236. [PubMed: 20299515]

Europe PMC Funders Author Manuscripts

Europe PMC Funders Author Manuscripts

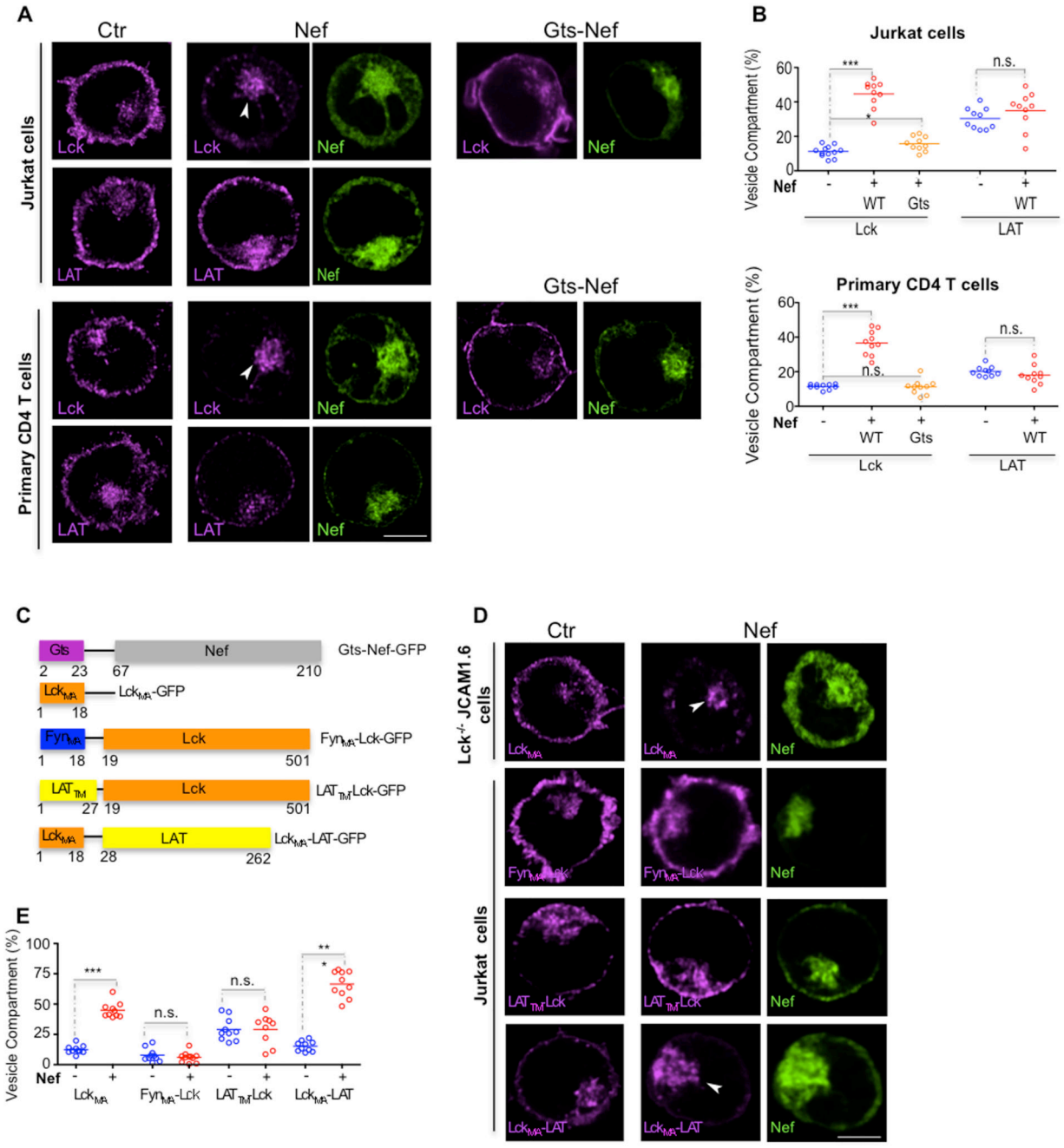

Figure 1. Nef promotes the vesicular retention of Lck but not of LAT.

(**A**) Deconvoluted confocal images of the effect of Nef and Gts-Nef (green) on the subcellular distribution of endogenous Lck and LAT (magenta) in Jurkat T cells (top panel) and in primary CD4 T cells (bottom panel).

(**B**) Population analysis quantifying the 3D fluorescence intensity in the vesicular compartment relative to total fluorescence of Lck and LAT in Jurkat cells (top panel) and in primary CD4 T cells processed as in (A) for n=10 cells per experimental condition.

(**C**) Schematic representation of the chimeric proteins used. To alter Nef trafficking properties its membrane anchoring domain was replaced by a Golgi targeting sequence (18). To alter Lck trafficking properties its membrane anchoring domain (Lck_{MA}) was replaced either with Fyn membrane anchoring domain (Fyn_{MA}-Lck) or with LAT transmembrane domain (LAT_{TM}-Lck). To alter LAT trafficking properties its transmembrane domain was replaced by Lck membrane anchoring domain (Lck_{MA}-LAT).

(**D**) Deconvoluted confocal images of the effect of Nef (green) on the subcellular distribution of Lck anchoring domain in Lck deficient JCAM1.6 cells (top row) and on Lck and LAT chimeric proteins (bottom rows) in Jurkat T cells.

(**E**) Population analysis quantifying the effect of Nef on the subcellular distribution of endogenous and chimeric Lck and LAT proteins, measured by 3D fluorescence intensity in the vesicular compartment relative to total fluorescence, in Jurkat T cells for n≥9 cells per experimental condition.

Arrows (**A**, **D**) highlight accumulation of the signaling molecules in the vesicular compartment; scale bar, 5 μm. Each symbol represents a cell. Data are representative (**A, D**) or represent (**B, E**) 3 independent experiments ***P<0.0001, n.s. not significative (Mann-Whitney test).

Europe PMC Funders Author Manuscripts

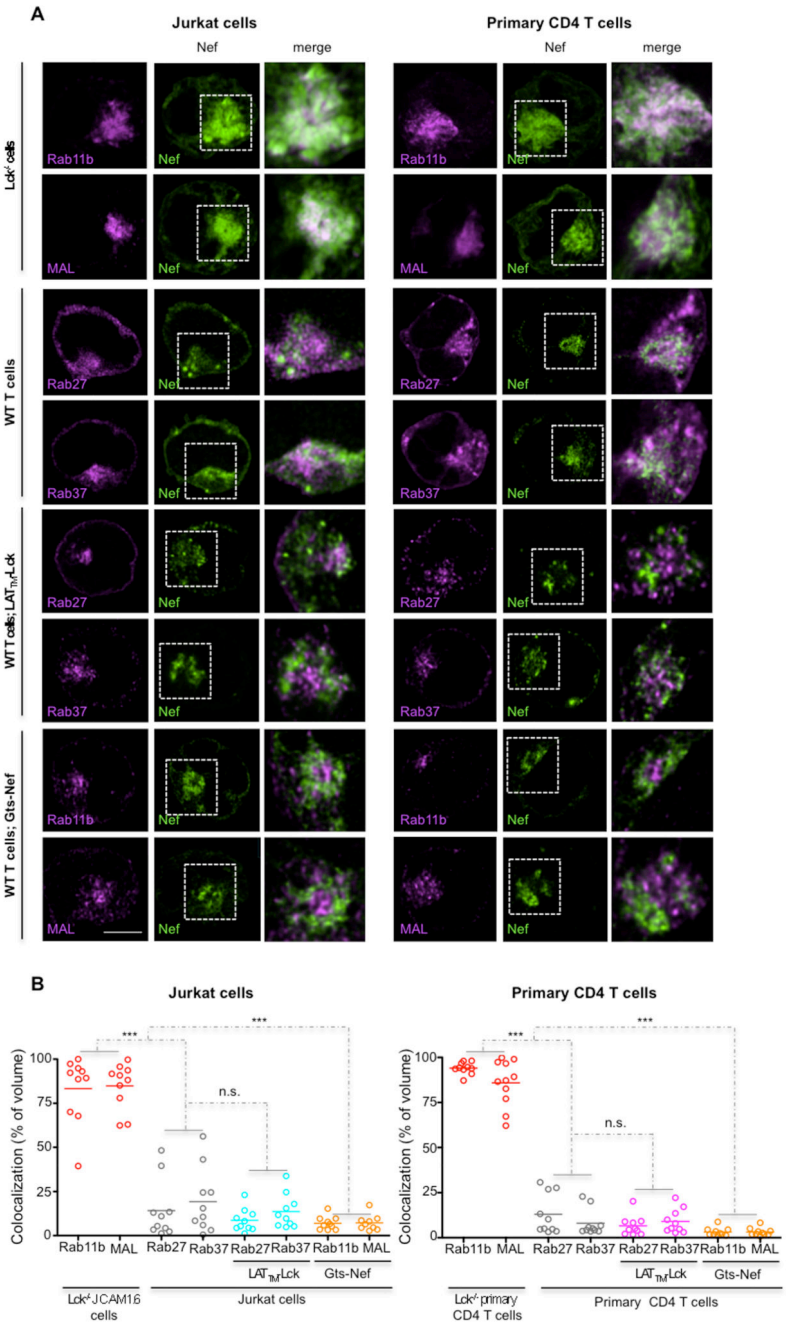

Figure 2. Nef selectively colocalizes with Lck traffic regulators Rab11b and MAL.

(A) Deconvoluted confocal images of Jurkat and primary T cells illustrating the degree of Nef co-localization (in white) with: top panel, the Lck traffic regulators Rab11b/MAL in Lck deficient JCAM1.6 and in primary CD4 T cells; and, middle panels, with the LAT traffic regulators Rab27/Rab37 in cells co-expressing or not LAT_{TM}-Lck. Bottom panels show the degree of Gts-Nef colocalization with the Lck traffic regulators Rab11b/MAL. Right images show inset amplification.

(**B**) Population analysis of the volume of co-localization in cells treated as in (A) for n=10 per experimental condition.

Europe PMC Funders Author Manuscripts

Europe PMC Funders Author Manuscripts

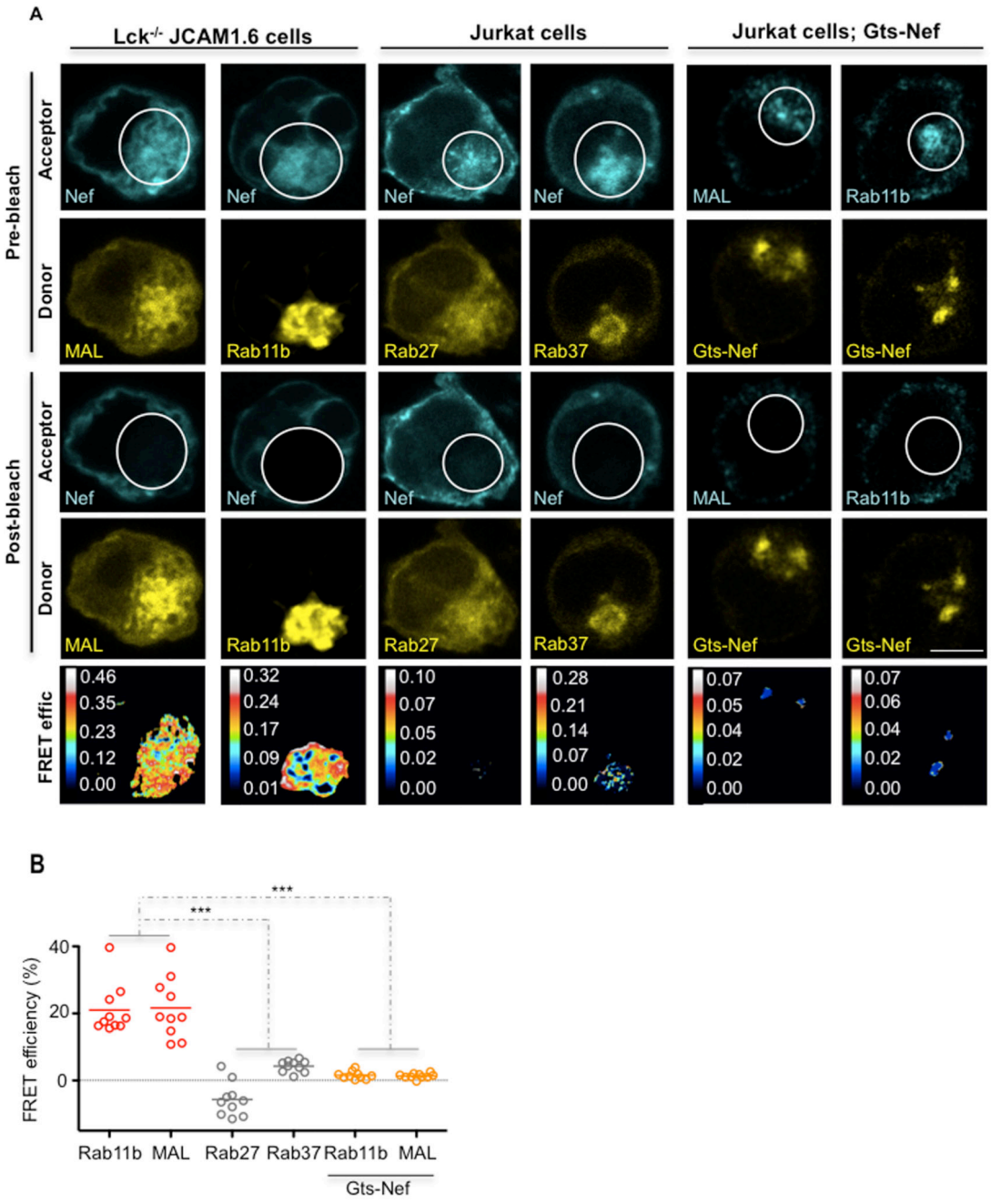

Figure 3. Nef selectively associates with the regulators of Lck vesicular traffic Rab11b and MAL.

(**A**) FRET imaging of Lck-deficient JCAM1.6 or Jurkat vesicular compartments by acceptor photobleaching. Top, imaging prior to photobleaching of the mCherry-tagged FRET-acceptors (Pre-bleach; Acceptor) and of the GFP-tagged FRET-donors (Pre-bleach; Donor). Middle, imaging post photobleaching of the mCherry-tagged FRET-acceptors (Post-bleach; Acceptor) and of the GFP FRET-donors (Post-bleach; Donor). Bottom panels display calculated [($Donor_{final}$-$Donor_{initial}$)/$Donor_{final}$] FRET efficiency maps. Bleached areas are indicated by white circles.

(**B**) Population analysis of FRET efficiencies for n=10 per experimental condition. Each symbol represents a cell. Scale bar, 5 μm. Data are representative (**A, B, D**) or represent (**C, E**) 2 independent experiments ***$P \leq 0.0001$; n.s. not significative (Mann-Whitney test).

Europe PMC Funders Author Manuscripts

Europe PMC Funders Author Manuscripts

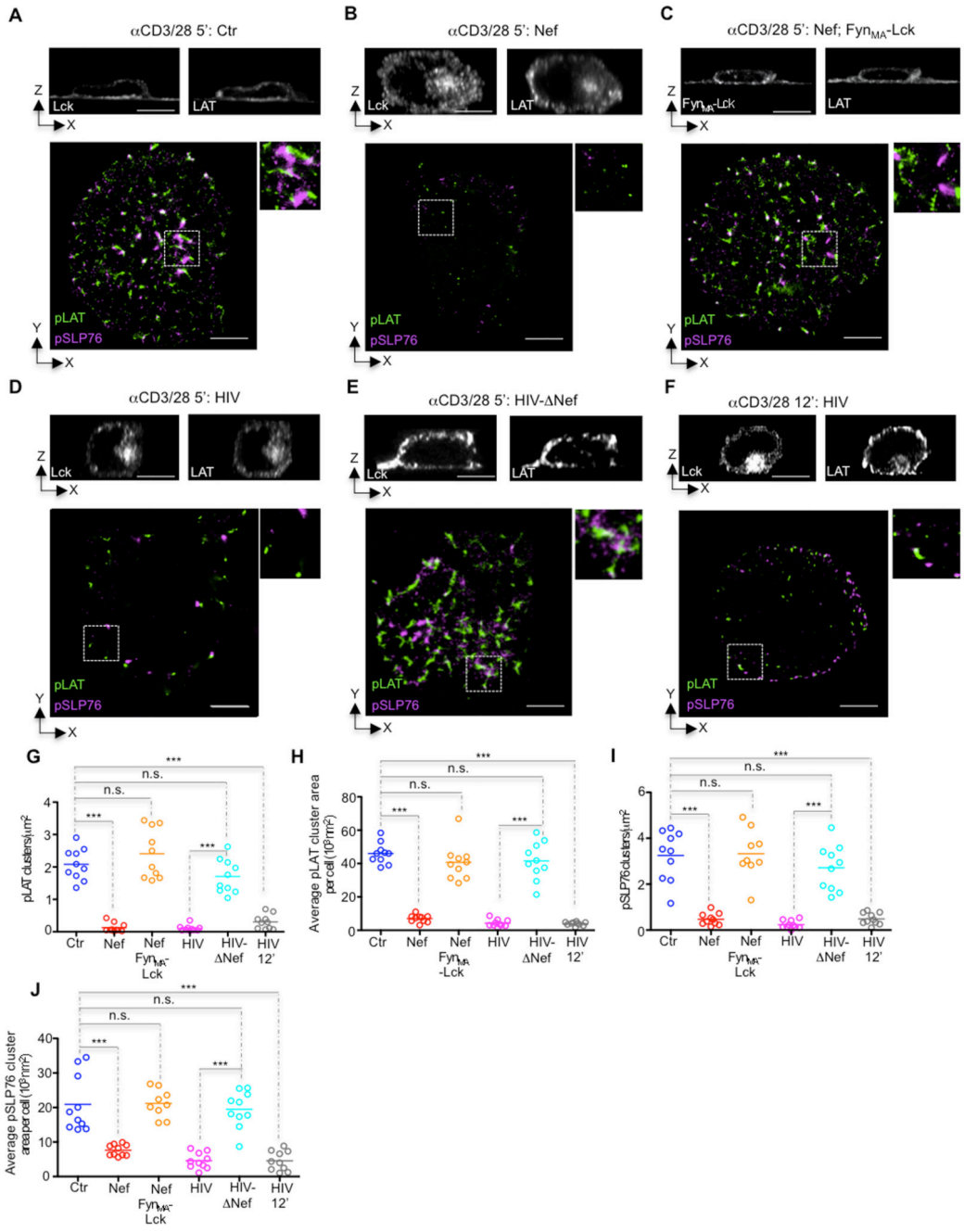

Figure 4. Nef co-opts the switch-like function of synaptic Lck in promoting TCR signal amplification.

(**A-F**) Top, confocal orthogonal view and bottom, *d*STORM-TIRF images of control (**A**), Nef expressing (**B**), Nef and Fyn$_{MA}$-Lck co-expressing (**C**), HIV **(D, F)**, or HIV-ΔNef infected **(E)** Jurkat cells fixed while interacting with glass coated with antibodies against CD3 and CD28 (CD3/28) for 5 min (**A-E**) or 12 min (**F**) and immunostained for Lck and/or LAT (top) or for pLAT (green) and pSLP76 (magenta) (bottom).

(**G**-**J**) Population analysis quantifying the effect of Nef on (**G**) the number of clusters of pLAT per square micrometer, (**H**) the mean pLAT cluster area per cell, (**I**) the number of clusters of pSLP76 per square micrometer and (**J**) the mean pSLP76 cluster area per cell, measured by super-resolution microscopy in cells treated as in (**A**-**F**) for n≥9 cells per experimental condition.

Each symbol represents a cell. Scale bar 5 μm. Data are representative (**A**-**E**) or represent (**G**-**J**) 2 independent experiments.

Europe PMC Funders Author Manuscripts

Europe PMC Funders Author Manuscripts

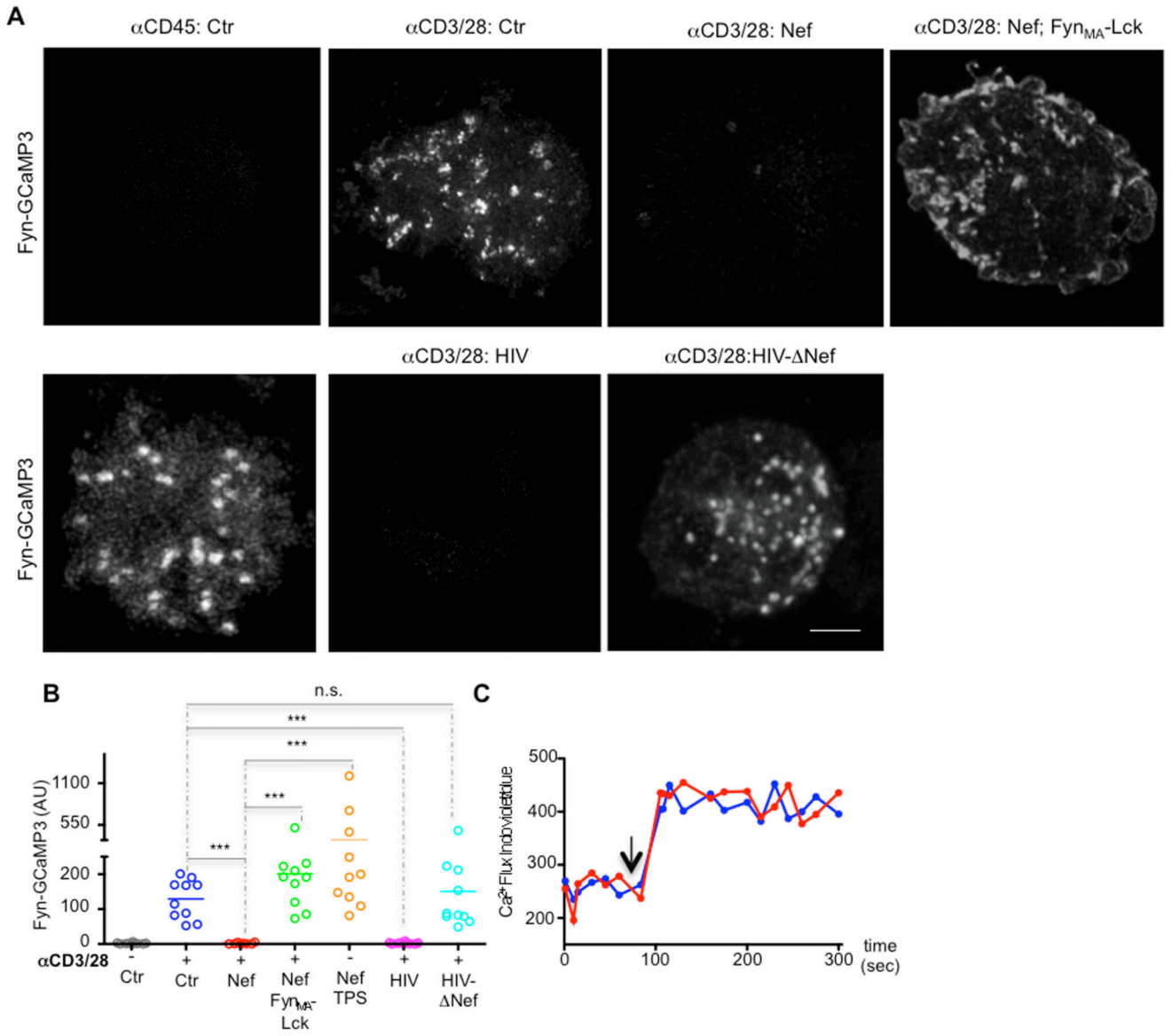

Figure 5. Nef impairs the formation of Ca^{2+} territories at the synaptic membrane.

(**A**) The membrane tethered and genetically encoded Ca^{2+} indicator (Fyn-GCaMP3) was used to image the formation of Ca^{2+} territories at the synaptic membrane of control, Nef expressing (Nef), Nef and Fyn_{MA}-Lck co-expressing (Nef; Fyn_{MA}-Lck), HIV or HIV-ΔNef infected Jurkat cells while interacting with glass coated with antibodies against CD3 and CD28 (αCD3/28) or with αCD45 (αCD45; Ctr) for 3 min before imaging.

(**B**) Population analysis of the formation Ca^{2+} membrane domains at the immunological synapse in Jurkat cells processed as in (**A**) (arbitrary units).

(**C**) Cytosolic Ca^{2+} flux measurements (showing the ratio of indo-blue to indo-violet) in control (blue) and Nef-expressing (red) Jurkat cells stimulated with ionomycin (arrow). Each symbol represents a cell. Scale bar 5 μm. Data are representative (**A, C**) or represent (**B**) 3 independent experiments ***$P \leq 0.0001$; n.s. not significative (Mann-Whitney test).

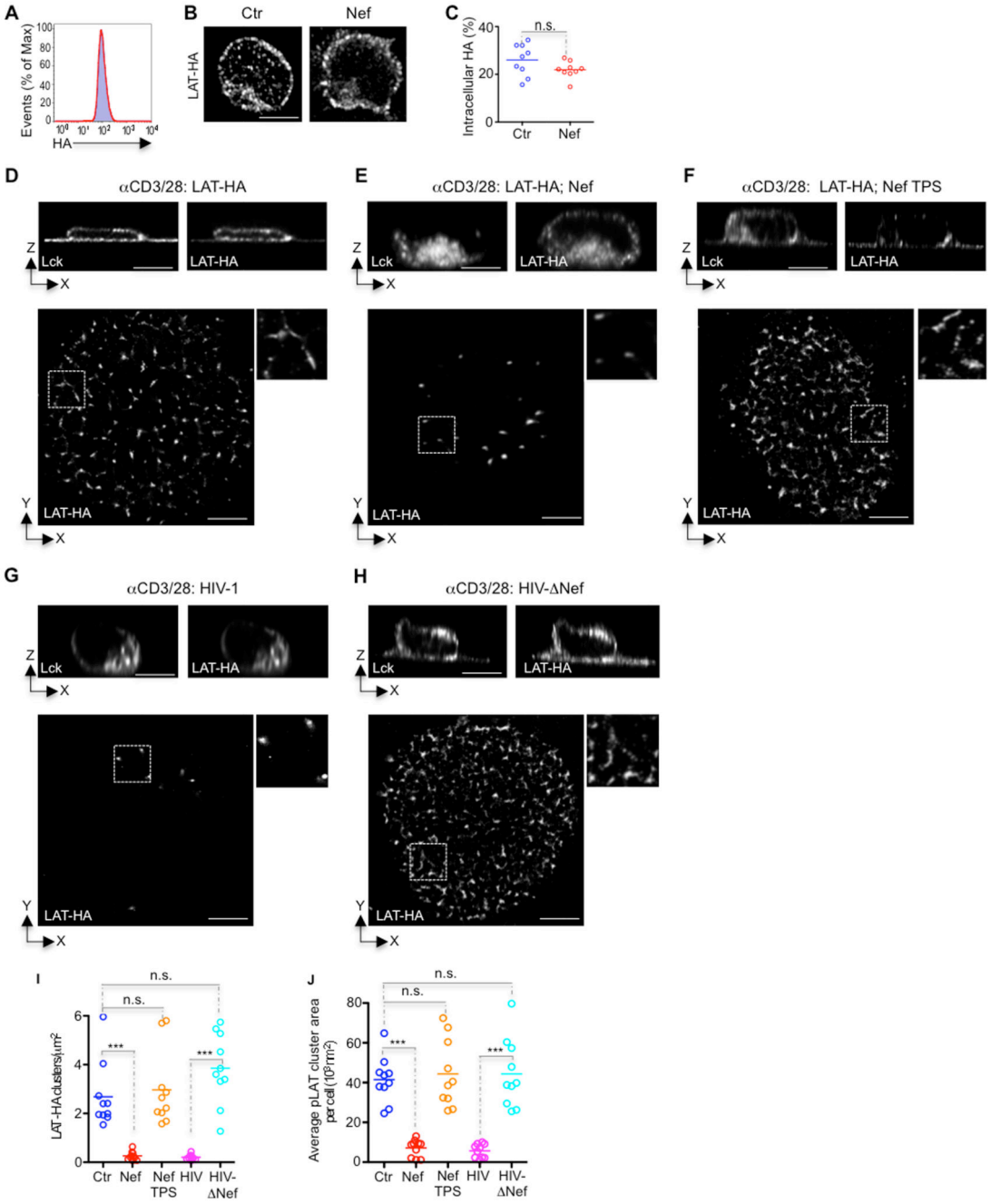

Figure 6. Nef impairs the formation of Ca^{2+} membrane territories controlling the signaling nanoarchitecture at the immunological synapse.

(**A**) Cytofluorimetry of the expression of LAT-HA in control (blue shaded histogram) and Nef-expressing Jurkat cells (red line) and labeled with mAb to HA.

(**B**) Deconvoluted confocal images illustrating the absence of Nef effect on the subcellular distribution of LAT-HA.

Europe PMC Funders Author Manuscripts

(**C**) Population analysis quantifying the absence of Nef effect on the subcellular distribution of LAT-HA, measured by 3D fluorescence intensity in the vesicular compartment relative to total fluorescence.

(**D**-**H**) Top, orthogonal view and bottom, *d*STORM-TIRF images of control (Ctr) (**D**), Nef transfected (Nef) (**E**), Nef-transfected and thapsigargin treated (Nef TPS) (**F**), HIV-1 infected (HIV) (**G**), or HIV-1 ΔNef infected (HIV-ΔNef) (**H**) Jurkat cells expressing LAT-HA, fixed while interacting with glass coated with antibodies against CD3 and CD28 for 5 min and immunostained for Lck and HA (top) or surface LAT-HA nanoclusters (bottom).

(**I, J**) Population analysis quantifying the effect of Nef on (**I**) the number of clusters of LAT-HA at the synaptic membrane per square micrometer and (**J**) the mean area of LAT-HA cluster at the synaptic membrane for n=10 cells per experimental condition, measured by super-resolution microscopy in cells treated as in (**D**-**H**, bottom).

Each symbol represents a cell. Scale bar 5 μm. Data are representative (**A**, **B**, **D**-**H**) or represent (**C, I, J**) 3 independent experiments ***$P \leq 0.0001$; n.s. not significative (Mann-Whitney test).